

Fumed-Alumina-Derived Nanoporous Alumina as a New Low-k Dielectric Material for Microelectronics Packaging

Yoshihiro Takizawa & D. D. L. Chung

Journal of Electronic Materials

ISSN 0361-5235

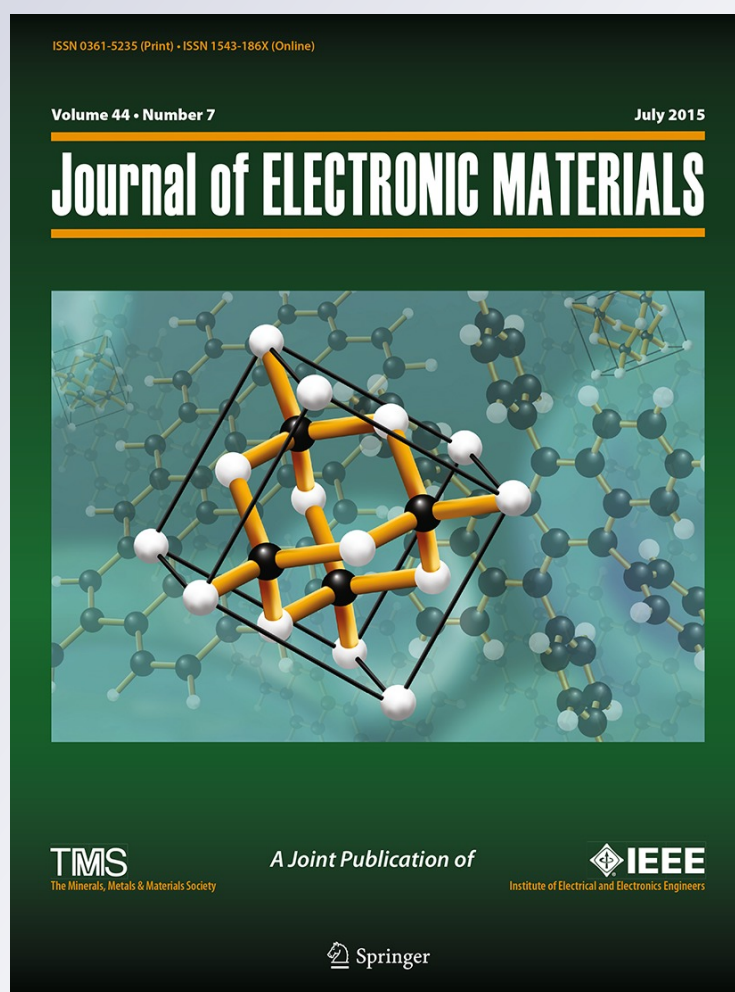
Volume 44

Number 7

Journal of Elec Materi (2015)

44:2211-2220

DOI 10.1007/s11664-015-3667-y



Your article is protected by copyright and all rights are held exclusively by The Minerals, Metals & Materials Society. This e-offprint is for personal use only and shall not be self-archived in electronic repositories. If you wish to self-archive your article, please use the accepted manuscript version for posting on your own website. You may further deposit the accepted manuscript version in any repository, provided it is only made publicly available 12 months after official publication or later and provided acknowledgement is given to the original source of publication and a link is inserted to the published article on Springer's website. The link must be accompanied by the following text: "The final publication is available at link.springer.com".



Fumed-Alumina-Derived Nanoporous Alumina as a New Low- k Dielectric Material for Microelectronics Packaging

YOSHIHIRO TAKIZAWA¹ and D.D.L. CHUNG^{1,2,3}

1.—Composite Materials Research Laboratory, University at Buffalo, State University of New York, Buffalo, NY 14260-4400, USA. 2.—e-mail: ddchung@buffalo.edu. 3.—URL: <http://alum.mit.edu/www/ddchung>

Dielectric materials with low relative dielectric constants (low- k dielectrics) are needed for electrical insulation to reduce signal propagation delay in microelectronics packaging. This paper reports use of nanoporous alumina of pore size mainly <50 nm and relative dielectric constant 2.0 (measured at frequencies from 100 kHz–2 MHz). Both values are lower than those previously reported. The material is innovatively made by compacting aggregates of submicron particles of fumed alumina. On compaction at 200 kPa, the aggregates are squashed, resulting in mechanical interconnection among the aggregates and formation of a nanostructured sheet with porosity 88%. Because the compacted material is, electrically, equivalent to solid alumina and air in parallel, its relative dielectric constant is 9, that of solid alumina. Reducing the pressure from 200 kPa to 50–100 kPa results in greater porosity (92–93%) and higher relative dielectric constant (2.0–2.3) for the compacted material, in addition to higher relative dielectric constant (13–21) for the solid alumina (because of the increase in the surface capacitance associated with surface charges). For a compaction pressure of 200 kPa, the thermal conductivity of the compacted material is 0.134 W/(m·K) and the upper bound of the thermal conductivity of the solid alumina is 0.94 W/(m·K). The fumed alumina is moldable by compaction.

Key words: Low- k dielectric, dielectric constant, permittivity, thermal conductivity, alumina, porous

INTRODUCTION

Dielectric materials with low relative dielectric constants (known as low- k dielectrics^{1,2}) are urgently needed as substrates, for inter-level insulation³ and for intra-level insulation⁴ in microelectronics, for the purpose of minimizing signal propagation delays. The lowest reported relative dielectric constant, 1.7, is that of porous polymers.^{1,2} Among ceramics, the lowest reported value is 2.2 (that of porous carbon-doped silicon oxide, i.e., organosilicate, in the form of a thin film with porosity 27%⁵). Ceramics tend to be superior to polymers in terms of thermal conductivity and ability to withstand elevated temperatures. Porosity reduces the relative dielectric constant but also reduces thermal conductivity, which is

important for heat dissipation in microelectronics. For example, for a carbon-doped silicon oxide with a relative dielectric constant of 2.3, the thermal conductivity is only 0.08 W/(m·K).⁶

Alumina (aluminium oxide, Al₂O₃) is one of the most widely used dielectric materials, although its relative dielectric constant is high (8.5⁷) in the absence of porosity. Porous alumina with 75% porosity and relative dielectric constant 2.4, as prepared by electrochemical anodization of aluminium then chemical etching, has been reported.⁴ The value of 2.4 is higher than that for porous carbon-doped silicon oxide, 2.2.⁵ The relative dielectric constant of 2.4⁴ for porous alumina can be reduced by increasing the porosity beyond 75%. A challenge in this process is the pore size, which must be sufficiently small for adequate insulation and mechanical performance.

(Received October 17, 2014; accepted January 24, 2015; published online February 26, 2015)

In this paper we report preparation of nanoporous alumina with a relative dielectric constant as low as 2.0. The value of 2.0 is lower than any previously reported for porous ceramics. This material differs from previously reported porous alumina^{3,4} in both structure and method of fabrication. The porosity is up to 88% in this work, compared with 75% in previous work.^{3,4} The pore size is mainly <50 nm in this work, compared to 50–100 nm in previous work.^{3,4}

The novel fabrication process involves compaction of fumed alumina, which is in the form of aggregates of nanoparticles. The aggregate structure is similar to that of carbon black. On compaction, the aggregates are squashed, resulting in mechanical interlocking among the particles and formation of a sheet, such that the shape of the sheet is determined by the shape of the surface used for compaction. This process is simpler, more environmentally friendly, and less expensive than the method involving chemical etching of alumina.⁴

The mechanical interlocking mentioned above results in a sheet with relatively high thermal conductivity, in addition to mechanical integrity in the absence of a binder, which tends to reduce the thermal conductivity. The mechanical interlocking and the absence of a binder are both attractive for enhancing thermal conductivity. Because the thermal conductivity decreases with increasing porosity,⁶ achievement of relatively high thermal conductivity at high porosity is a challenge.

A porous material consists of a solid part and air. The relative dielectric constant of a porous material is determined by that of the solid part and by the porosity. For the purpose of basic understanding, it is valuable to obtain the relative dielectric constant of the solid part. In particular, it is useful to know how this value depends on processing conditions and how it compares with the literature value for the 100% dense solid. The relative dielectric constant of the solid part has not been addressed in previous work.^{1–6} Measurement of the relative dielectric constant of a material involves measurement of capacitance, with the specimen sandwiched between conductor plates. However, the measured capacitance includes the contributions from the specimen and each of the two interfaces between the specimen and the conductor plates, such that the specimen and the two interfaces are three capacitances in series. Hence, the measured capacitance C is given by the equation:

$$1/C = 2/C_i + L/(\epsilon_0 \kappa A), \quad (1)$$

where C_i is the capacitance of a specimen–conductor interface, ϵ_0 is the permittivity of free space (8.85×10^{-12} F/m), κ is the relative dielectric constant of the specimen, A is the contact area, and L is the thickness of the specimen. As shown by Eq. 1, C_i should be high for it to have little effect on C . Previous work^{1–6} has neglected the interface contributions. As

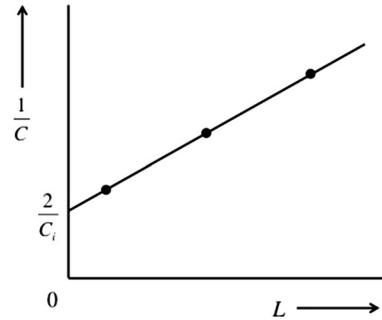


Fig. 1. Schematic diagram of a plot of $1/C$ as a function of L for determination of C_i and κ on the basis of Eq. 1, where C_i is the capacitance of a specimen–conductor interface, κ is the relative dielectric constant of the specimen, and L is the thickness of the specimen. The slope is $1/(\epsilon_0 \kappa A)$ and the intercept on the vertical axis is $2/C_i$.

a consequence, the last term in Eq. 1 is overestimated, and thus κ is underestimated. This means that previously reported values of the relative dielectric constant of low- k dielectrics are underestimated. In contrast, this work does not neglect the interface contributions. By measuring C for specimens at three or more thicknesses, the interface and specimen contributions are isolated. According to Eq. 1, $1/C$ is plotted against l , as illustrated in Fig. 1. The value of C_i is obtained from the intercept of $2/C_i$ with the $1/C$ axis at $l = 0$, and the value of κ is obtained from the slope, which is $1/(\epsilon_0 \kappa A)$. This method of isolation has previously been used to study carbon materials.⁸ The more accurate measurement of the specimen capacitance enabled by this isolation, enables meaningful analysis of the specimen's relative dielectric constant. The analysis, as performed in this work, gives the relative dielectric constant of the solid part of the porous material.

The objectives of this work were:

1. To obtain a low- k dielectric material in the form of a ceramic (nanoporous alumina) with a relative dielectric constant as low as 2.0;
2. To obtain a low- k dielectric material with thermal conductivity higher than the previously achieved value of 0.08 W/(m·K) for porous carbon-doped silicon oxide with porosity 33% and relatively dielectric constant 2.3;⁶
3. To develop a cost-effective and environmentally friendly method for fabrication of highly porous low- k alumina;
4. To analyze the relative dielectric constant and thermal conductivity of the porous low- k alumina, to enable determination of the corresponding values of the solid part of the porous alumina; and
5. To isolate the contributions of the specimen and the specimen–conductor interface to the measured capacitance, to enable accurate determination of the relative dielectric constant of the specimen.

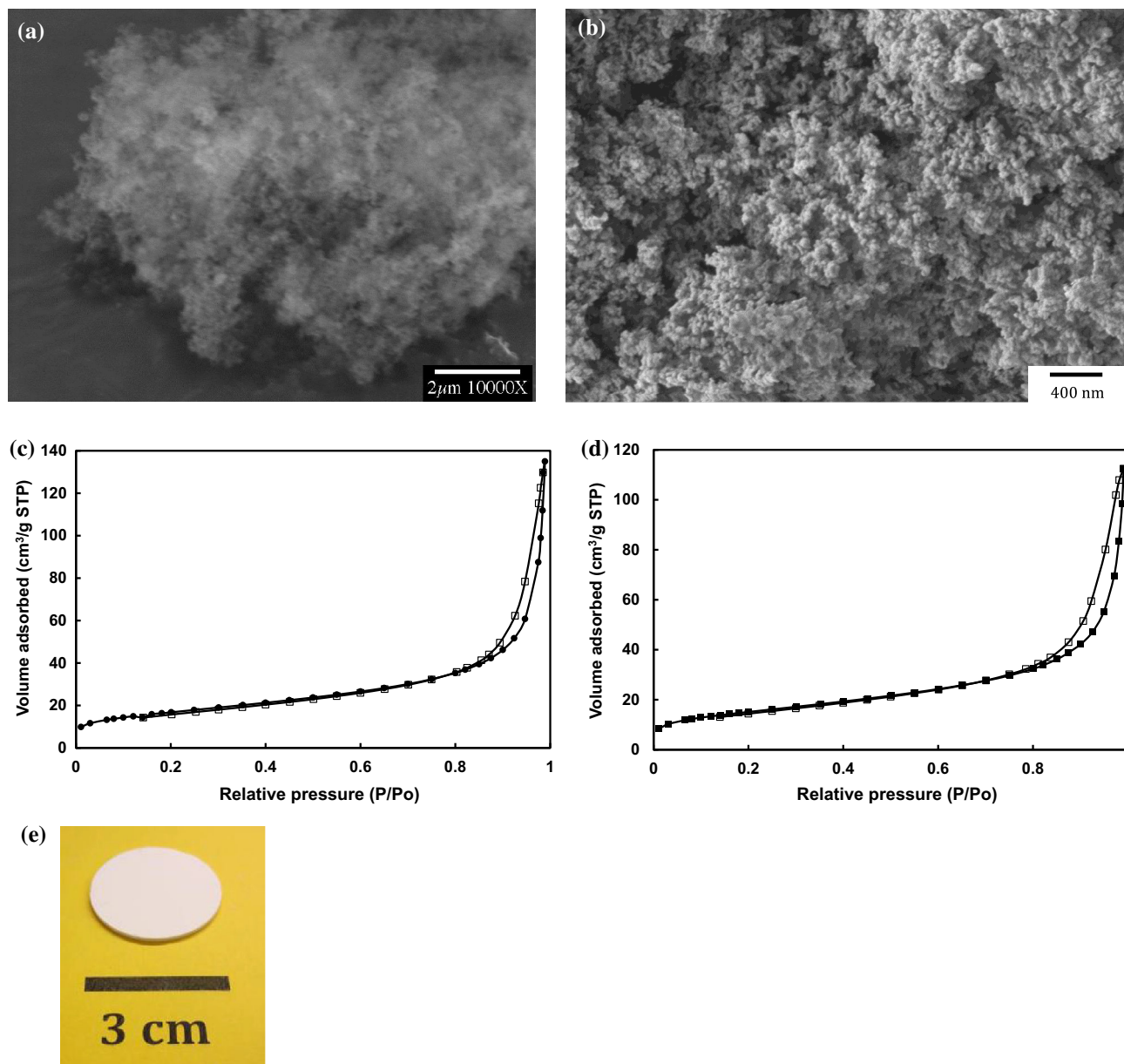


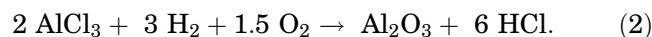
Fig. 2. Structure of fumed alumina before and after compaction. (a) SEM photograph of the fumed alumina before compaction. (b) SEM photograph of fumed alumina after compaction, with the view being the plane perpendicular to the direction of compaction. The microstructure is the same as in the view of the side plane that contains the direction of compaction. (c) Adsorption-desorption isotherms of fumed alumina before compaction, with the lower curve being the adsorption curve and the upper curve being the desorption curve. (d) Adsorption-desorption isotherms of fumed alumina after compaction at 200 kPa, with solid symbols for the adsorption curve and open symbols for the desorption curve. (e) Digital-camera optical photograph of a disk of compacted fumed alumina fabricated by compaction at 200 kPa.

EXPERIMENTAL

Materials

The fumed alumina used, marketed as SpectraAl 51 by Cabot (Billerica, MA, USA), was in its untreated state. It is a white fluffy powder of specific gravity 3.6 at 20°C and melting point approximately 2000°C. In contrast with conventional alumina, fumed alumina is produced in a flame. The reaction involved is proprietary according to the

manufacturer, but a reaction⁹ commonly used for making fumed alumina is:



In this reaction, aluminium chloride, hydrogen, and oxygen are the reagents. The material obtained is in the form of aggregated nanoparticles with specific surface area 55 m²/g, aggregate size 100–200 nm, Al₂O₃ content exceeding 99.8 wt.%, and a positive

surface charge. The positive charge is probably because of dissociation of ionogenic groups on the particle surface and/or differential adsorption from solution of ions of different charge by the surface during fabrication of the fumed alumina. The aggregates form loose, micrometer-sized agglomerates. The mass loss on heating is less than 1.5 wt.% at 105°C. The fumed alumina is a mixture of theta, delta, gamma, and amorphous forms of alumina. Its morphology is shown by the scanning electron microscope (SEM) photograph in Fig. 2a. Because of the porous aggregate structure, the fumed alumina is squashable (highly deformable) on compression. It has previously been used as the solid component of a thermal paste.¹⁰ The performance of the thermal paste is excellent, because of the squashability of the fumed alumina and the consequent conformability of the paste.^{10,11} More commonly, fumed alumina is used in the formulation of polymer-based coatings.

Measurement of Relative Dielectric Constant

A known amount, by mass, of fumed alumina powder was placed in an electrically nonconducting polymer cylinder (inner diameter 31.8 mm, height 60 mm) such that it was sandwiched inside the cylinder by two pieces of copper foil (each of diameter 31.7 mm and thickness 0.127 mm), which served as electrical conductors for measurement of the relative dielectric constant. Before introduction of the fumed alumina, each piece of foil was bonded to an epoxy piston of diameter 31.7 mm and height 15 mm, during fabrication of the piston from epoxy resin. Each piece of copper foil had an integral extended part that protruded beyond the circular main part of the copper foil, to serve as an electrical connection. A controlled load (a known weight that fits inside the cylinder) was applied via the upper piston for the purpose of compacting the fumed alumina. The thickness of the resulting compacted alumina was obtained by measuring the vertical distance between the top rim of the cylinder and the top surface of the upper piston. For each value of the load, compacted alumina of three thicknesses was obtained by use of three different amounts of fumed alumina. Four pressures (corresponding to four loads) were used, 50, 75, 100, and 200 kPa. For example, at the pressure of 200 kPa, the three thicknesses were 0.8, 1.2 and 1.6 mm; at the pressure of 50 kPa, the three thicknesses were 1.6, 2.1, and 2.7 mm. By using three thicknesses, the specimen and interface contributions to the measured capacitance were isolated, as illustrated in Fig. 1.

Without removing the compacted alumina from the cylinder, the relative dielectric constant was measured by use of a precision RLC meter (Quadtech 7600; Marlborough, MA, USA). The compaction pressure was maintained during the measurement, which involves measuring the capacitance at different frequencies that are scanned from 10 Hz to 2 MHz. The AC voltage applied between the two

pieces of copper foil ranged from 300 mV to 1.000 V, so the resulting AC electric field was fixed at 3.7 V/cm.

Measurement of Thermal Conductivity

Fumed alumina powder was positioned between two polytetrafluoroethylene (PTFE) sheets inside a stainless steel cylinder (inner diameter 31.7 mm, height 79 mm). The steel cylinder was fitted with a stainless steel cylindrical piston positioned above the upper PTFE sheet. A compressive pressure of 200 kPa was applied, by use of the piston, to compact the fumed alumina. The resulting compacted alumina (specimen) was removed from the steel cylinder and placed between two copper cylinders that were parts of the equipment used for measurement of thermal conductivity (Fig. 3). No thermal paste was used between the specimen and either copper cylinder.

Thermal conductivity was measured by use of the guarded hot plate method, a steady-state method commonly used for measurement of the through-thickness thermal conductivity of specimens in sheet form.¹⁰ (This is in contrast with transient methods.¹²) In this work, the specimen (positioned horizontally) was sandwiched between a pair of copper cylinders (one cylinder was connected to a

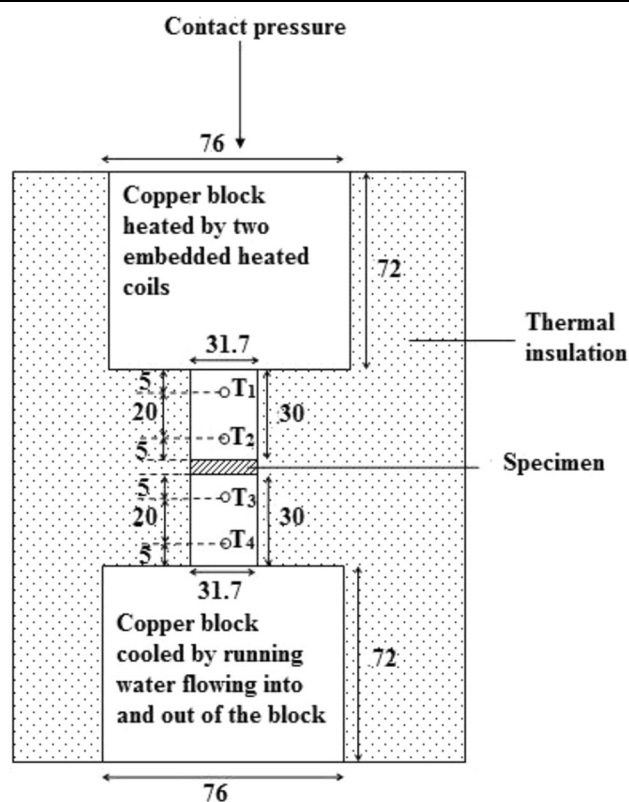


Fig. 3. Schematic illustration of the guarded hot plate experimental equipment used for measurement of thermal conductivity. The specimen was sandwiched between two copper cylinders, and the temperature gradient was determined by measuring the temperatures T_1 , T_2 , T_3 , and T_4 . All dimensions are in millimeters.

heated block, the other to a cooled block), as illustrated in Fig. 3. The roughness of the copper sandwiching surfaces was $15\ \mu\text{m}$, achieved by mechanical polishing. The vertical sides of the specimen, cylinders, and blocks were thermally insulated so heat flow was essentially one-dimensional (vertical). The measured thermal resistance (which is related to the temperature drop) was that between the surfaces of the blocks that sandwich the specimen. This measured thermal resistance was the sum of the thermal resistance of the specimen and that of each of the two interfaces between the specimen and the two blocks. To isolate the contributions of specimen and the interface to the measured thermal resistance, measurement was performed on specimens with three different thicknesses, as explained below.

The total thermal resistance R_t is given by:

$$R_t = R_s + 2R_i, \quad (3)$$

where R_s is the thermal resistance of the specimen and R_i is the thermal resistance of the interface between the specimen and a sandwiching surface. The total thermal resistance is the inverse of the thermal contact conductance divided by the area of the heat conduction path, A . The thermal resistance, R_s , of the specimen can be written as:

$$R_s = \frac{L}{\sigma A}, \quad (4)$$

where σ is the thermal conductivity of the specimen and L is the thickness of the specimen. Therefore, on the basis of Eq. 3, the thermal resistivity is given by:

$$R_t A = \frac{L}{\sigma} + 2R_i A. \quad (5)$$

Thus, σ is given by the inverse of the slope of the plot of thermal resistivity as a function of specimen thickness.

In Fig. 3, each of the two sandwiching copper cylinders is of height 30.0 mm and diameter 1.25 in (31.7 mm). Each cylinder contains two drilled blind holes (3.3 mm diameter) for insertion of thermocouples. The center of each circular hole is 5.0 mm from an end surface of the cylinder. The two holes in each cylinder, with the thermocouple, enable measurement of the temperature gradient in the cylinder. On the basis of the temperature gradient, the temperature at the end surface of the cylinder touching the specimen can be obtained by extrapolation. The temperatures at the lower surface of the specimen and the upper surface of the lower copper cylinder are the same. Similarly, the temperatures at the upper surface of the specimen and the lower surface of the upper copper cylinder are the same. Thus, the temperature gradient across the specimen is determined. A temperature gradient is imposed between the copper cylinders by use of two larger 3.00 in \times 3.00 in (76.0 mm \times

76.0 mm) square copper blocks. The block above the upper copper cylinder serves as a heat source, because it has embedded heating coils, such that the temperature is controlled by use of a temperature controller, with the temperature set at 100°C . The block below the lower copper cylinder serves as a cold block, because it is cooled by running water that flows into and out of the block. Thermal equilibrium is achieved when the temperature at every hole becomes stable. The entire equilibrium process takes approximately 1.0 h.

A contact pressure (120 kPa) was applied in the direction perpendicular to the plane of the specimen, by use of a screw-action load cell. The pressure was monitored by use of a calibrated attached strain gauge.

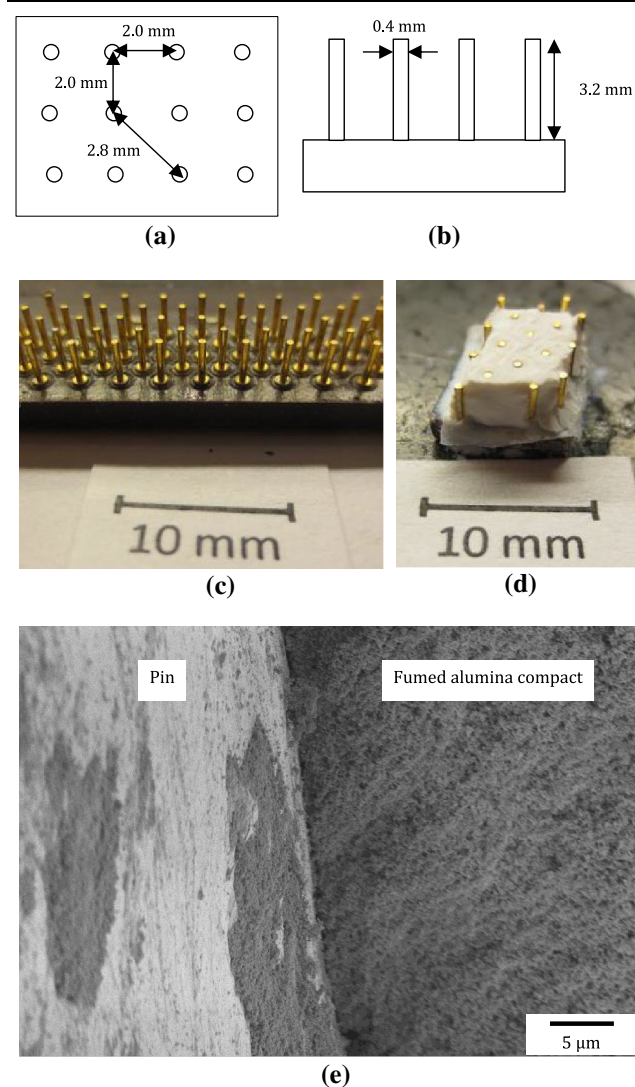


Fig. 4. (a) Top view of the pin grid array used for moldability testing. (b) Side view of the pin grid array. (c) Digital-camera optical photograph of pin grid array. (d) Digital-camera optical photograph of the compacted fumed alumina positioned among the pins of a pin grid array (a–c), demonstrating its moldability. (e) Side view showing the interface of the compacted alumina and a pin along the length of the pin. The pin is in the left half of the photograph.

For one-dimensional heat flow in this situation, the heat flow is the same in all parts of the conduction path; it can therefore be obtained from that in a copper cylinder. The heat flow, q , in a copper cylinder of thermal conductivity, σ , and cross-sectional area, A , because of a temperature gradient, $\Delta T/d_A$, is given by:

$$q = \frac{\Delta Q}{t} = \frac{\sigma A \Delta T}{d_A}, \quad (6)$$

where Q is the heat that flows over a time Δt , d_A is the distance (20.00 mm) between two holes in the cylinder, and ΔT is the temperature difference between these holes.

The temperature of the lower surface of the upper copper cylinder is given by the expression:

$$T_A = T_2 - \frac{d_B}{d_A} (T_1 - T_2). \quad (7)$$

where d_B is the distance between the upper surface of the specimen and thermocouple T_2 (5.00 mm) and d_A is the distance between thermocouples T_1 and T_2 (20.00 mm). Hence, $T_1 - T_2$ is the temperature difference over the distance d_A .

Similarly, the temperature of the upper surface of the lower copper cylinder is given by the expression:

$$T_D = T_3 + \frac{d_D}{d_C} (T_3 - T_4), \quad (8)$$

where d_D is the distance between the lower surface of the specimen and thermocouple T_3 (5.00 mm) and d_C is the distance between thermocouples T_3 and T_4 (20.00 mm). Hence, $T_3 - T_4$ is the temperature difference over the distance d_C . Because the two copper cylinders are identical, d_C is equal to d_A .

Because of the geometric symmetry of the two copper cylinders, Eqs. 7 and 8 can be simplified to:

$$T_A = T_2 - \alpha \Delta T, \quad (9)$$

and

$$T_D = T_3 + \alpha \Delta T, \quad (10)$$

where

$$\alpha = \frac{d_B}{d_A} = \frac{d_D}{d_C} = 0.25.$$

The thermal resistivity is given by:

$$\theta = (T_A - T_D) \frac{A}{q}. \quad (11)$$

By subtracting Eq. 10 from Eq. 9, substituting the result in Eq. 11 and then substituting q from Eq. 6 into Eq. 11, the thermal resistivity is obtained as:

$$\theta = \left(\frac{T_2 - T_3}{\Delta T} - 2\alpha \right) \frac{d_A}{\sigma}. \quad (12)$$

The thermal resistivity is independent of area, whereas thermal resistance depends on the area.

Moldability Testing

To test the moldability of the fumed alumina, fumed alumina (before compaction) was placed on top of a pin grid array (Fig. 4a–c) and then compressed from the top at a pressure of 200 kPa. The integrated circuit package is square, but only part of the array (as cut from the overall array) is used. During the compression, the pins of the array faced down toward the fumed alumina particles contained in a steel cylinder and the pressure was applied from the top by use of a steel piston.

Analysis of Microstructure

Measurement of specific surface area and pore size distribution was conducted by isothermal gas adsorption, by use of nitrogen and the Micromeritics ASAP 2010 physisorption analyzer. By measurement the volume of nitrogen adsorbed by a specimen at different pressures, total pore volume and surface area inside the specimen can be determined. The pore size distribution is inferred from the adsorption isotherm by use of the well-known Barrett–

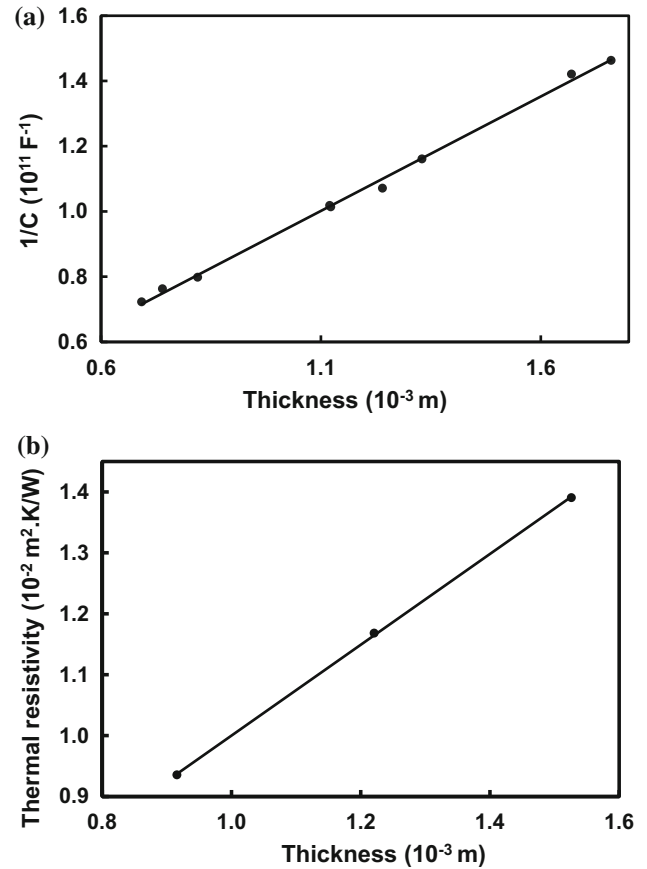


Fig. 5. (a) Plot of $1/C$ (where C is measured capacitance) as a function of specimen thickness for fumed alumina compacted at 200 kPa and tested at 2 MHz. (b) Plot of the thermal resistivity as a function of specimen thickness for fumed alumina compacted at 200 kPa. The thickness is obtained from the relationship between thickness and mass, which is the controlled quantity in the experiment.

Table I. Relative dielectric constant of fumed alumina compacted at different pressures and tested at different frequencies

Compaction pressure (kPa)	Volume fraction		Relative dielectric constant			
	Solid	Air	100 kHz	200 kHz	1.00 MHz	2.00 MHz
50	0.066 ± 0.004	0.934 ± 0.004	2.17 ± 0.14 ^a <i>18.7 ± 1.1^b</i>	2.25 ± 0.14 ^a <i>19.9 ± 1.0^b</i>	2.31 ± 0.10 ^a <i>20.8 ± 0.3^b</i>	2.35 ± 0.11 ^a <i>21.4 ± 0.4^b</i>
75	0.071 ± 0.006	0.929 ± 0.004	2.10 ± 0.12 ^a <i>16.5 ± 0.1^b</i>	2.17 ± 0.13 ^a <i>17.4 ± 0.2^b</i>	2.10 ± 0.15 ^a <i>16.4 ± 0.5^b</i>	2.13 ± 0.14 ^a <i>16.9 ± 0.4^b</i>
100	0.082 ± 0.008	0.918 ± 0.008	2.03 ± 0.11 ^a <i>13.5 ± 0.1^b</i>	2.02 ± 0.08 ^a <i>13.5 ± 0.2^b</i>	2.00 ± 0.10 ^a <i>13.2 ± 0.0^b</i>	2.00 ± 0.13 ^a <i>13.2 ± 0.4^b</i>
200	0.122 ± 0.015	0.878 ± 0.015	1.97 ± 0.17 ^a <i>8.90 ± 0.42^b</i>	2.01 ± 0.12 ^a <i>9.28 ± 0.03^b</i>	2.03 ± 0.06 ^a <i>9.51 ± 0.55^b</i>	2.04 ± 0.04 ^a <i>9.61 ± 0.73^b</i>

Shown in italics is the relative dielectric constant (κ') of the solid alumina part of the compacted alumina.^aRelative dielectric constant of the compacted alumina.^bRelative dielectric constant (κ') of the solid alumina part of the compacted alumina, as calculated from the measured relative dielectric constant of the sample by use of the rule of mixtures, with the solid alumina and air being electrically in parallel. The dielectric constant of air is 1.00.

Joyner–Halenda (BJH) method. In addition, SEM was conducted to observe pore morphology.

RESULTS AND DISCUSSION

Microstructure

Figure 2b shows that the pores in the compacted alumina were mainly less than 50 nm in size, although some exceed 100 nm, probably because of interfaces between fumed alumina aggregates. Nitrogen adsorption (Fig. 2c and d) shows that the specific surface area was $60.4 \pm 0.1 \text{ m}^2/\text{g}$ and $54.8 \pm 0.1 \text{ m}^2/\text{g}$ before and after compaction, respectively; the average pore size (by the BJH method, over the pore-size range from 1 nm to 200 nm) was 14.8 nm and 14.5 nm before and after compaction, respectively; the cumulative pore volume (by the BJH method, over the pore size range from 1 nm to 200 nm) was $0.213 \text{ cm}^3/\text{g}$ and $0.166 \text{ cm}^3/\text{g}$ before and after compaction, respectively. These observations mean that compaction only slightly reduces specific surface area and pore size. The hysteresis in the adsorption–desorption isotherms shows that the fumed alumina is mesoporous, with the occurrence of capillary condensation, both before and after compaction. The slightly larger adsorption–desorption hysteresis area after compaction is attributed to the consolidated structure after compaction, which hinders out-diffusion of desorbed gas.

Figure 2e shows a digital-camera optical image of compacted fumed alumina prepared by compaction at 200 kPa. The edges of the disk are sharp and the surface is smooth, because of the squashability and conformability of the fumed alumina.

Relative Dielectric Constant

Figure 5a shows a typical plot of $1/C$ as a function of specimen thickness for compacted fumed alumina. Linearity is observed for all the compaction

pressures and test frequencies, in accordance with Eq. 1.

Table I shows that, for any of the frequencies, the relative dielectric constant of compacted fumed alumina decreases with increasing solid volume fraction. This trend is unexpected. The air volume fraction is the same as the porosity. This means that the relative dielectric constant of the compacted alumina decreases with decreasing porosity. The solid volume fraction increases with increasing compaction pressure, as expected.

On the basis of the measured value of the relative dielectric constant of the compacted alumina, the relative dielectric constant (κ') of the solid alumina part of the compacted alumina is calculated on the basis of the rule of mixtures (with alumina solid and air regarded as electrically in parallel). The Maxwell–Wagner mixing rule¹³ did not give reasonable results. The capacitance of the solid alumina (C_a) is given by:

$$C_a = \frac{\epsilon_0 \kappa' A}{L} \quad (13)$$

where A is the cross-sectional area of the solid alumina and L is the thickness of the specimen, which is the same as that of the solid alumina. The area A is given by the volume divided by the thickness, with the volume being given by the mass divided by the density of ideal solid alumina (3.95 g/cm^3). Hence:

$$A = \frac{\text{Mass of fumed alumina (g)}}{\text{Density of solid alumina} \left(\frac{\text{g}}{\text{cm}^3} \right) \times \text{thickness (m)}} \quad (14)$$

Table I shows that the relative dielectric constant of the solid alumina decreases with increasing compaction pressure, i.e., decreases with decreasing

Table II. Surface capacitance of the solid alumina per unit mass, as obtained by considering the surface capacitance and volumetric capacitance as being in parallel

Frequency	Compaction pressure (kPa)	κ''	Surface capacitance of the solid alumina per unit mass (10^{-12} F/g)		
			1.5 mm	2.0 mm	2.5 mm
100 kHz	50	8.9 ± 1.6	11 ± 1^a	6.0 ± 0.4^a	3.9 ± 0.2^a
	75	9.3 ± 2.0	8.3 ± 0.6^a	4.7 ± 0.3^a	3.0 ± 0.2^a
	100	9.5 ± 0.0	5.0 ± 0.3^a	2.8 ± 0.2^a	1.8 ± 0.1^a
	200	9.6 ± 0.1	0^a	0^a	0^a
200 kHz	50	8.9 ± 0.4	9.7 ± 0.4^b	5.5 ± 0.3^b	3.5 ± 0.2^b
	75	9.3 ± 0.0	12 ± 1^a	6.5 ± 0.6^a	4.2 ± 0.4^a
	100	9.5 ± 0.6	8.9 ± 0.2^a	5.0 ± 0.1^a	3.2 ± 0.1^a
	200	9.6 ± 0.7	4.6 ± 0.2^a	2.6 ± 0.1^a	1.7 ± 0.1^a
1.00 MHz	50	8.9 ± 0.2	0^a	0^a	0^a
	75	9.3 ± 0.4	10 ± 0^b	5.7 ± 0.0^b	3.7 ± 0.0^b
	100	9.5 ± 0.6	12 ± 0^a	6.9 ± 0.2^a	4.4 ± 0.1^a
	200	9.6 ± 0.1	7.6 ± 1.2^a	4.2 ± 0.7^a	2.7 ± 0.4^a
2.00 MHz	50	8.9 ± 0.4	4.0 ± 0.7^a	2.3 ± 0.4^a	1.5 ± 0.2^a
	75	9.3 ± 0.0	0^a	0^a	0^a
	100	9.5 ± 0.6	10 ± 1^b	5.8 ± 0.4^b	3.7 ± 0.2^b
	200	9.6 ± 0.7	13 ± 0^a	7.3 ± 0.2^a	4.6 ± 0.1^a
			8.0 ± 1.2^a	4.5 ± 0.7^a	2.9 ± 0.4^a
			3.9 ± 0.3^a	2.2 ± 0.2^a	1.4 ± 0.1^a
			0^a	0^a	0^a
			11 ± 1^b	5.9 ± 0.4^b	3.8 ± 0.3^b

Results are given for three specimen thicknesses (1.5–2.5 mm) and four frequencies. Shown in italics is the volumetric capacitance of the solid alumina per unit mass, as obtained by considering the surface capacitance and volumetric capacitance as being in parallel. Shown in bold font is the relative dielectric constant (κ'') of the volume part of the solid alumina in compacted alumina; this quantity is independent of specimen thickness.^aSurface capacitance of the solid alumina per unit mass (10^{-12} F/g).^bVolumetric capacitance of the solid alumina per unit mass (10^{-12} F/g), as obtained by considering the surface capacitance and volumetric capacitance as being in parallel.

porosity. At the lowest porosity (88%, Table I), the value is essentially equal to the literature value for bulk alumina ($9.3^{14,15}$). At the highest porosity (92–93%, Table I), the value is higher than that of bulk alumina. This means that the solid alumina at the lowest porosity (88%) is similar in structure to bulk alumina, whereas the solid alumina at the highest porosity (92–93%) differs from bulk alumina in that it is more polarizable than bulk alumina. The extra polarizability is probably because of a surface contribution. Because of the nanostructure of the compacted fumed alumina, the surface area is substantial and the surface probably has functional groups which can interact with the applied AC electric field. The presence of functional groups is a consequence of the production of fumed alumina in a flame and is supported by the surface positive charge that is present, according to product information from Cabot.

To estimate this surface contribution, the capacitance C_a of the solid alumina is modeled as a volumetric contribution in parallel with a surface contribution. Hence:

$$C_a = \frac{\epsilon_o \kappa'' A}{L} + C_j \quad (15)$$

where $\epsilon_o \kappa'' A / L$ is the volumetric contribution and C_j is the surface contribution. In other words, κ'' is the

relative dielectric constant of the volume part of the solid alumina. The value of κ'' is taken as that of the solid alumina for the sample with the lowest porosity, because the relative dielectric constant of this solid alumina (last row of Table I) is essentially equal to that of ideal bulk alumina. Hence, combining Eqs. 13 and 15 gives:

$$C_j = \frac{\epsilon_o \kappa' A}{L} - \frac{\epsilon_o \kappa'' A}{L} = \frac{\epsilon_o A}{L} (\kappa' - \kappa'') \quad (16)$$

Use of a series model for the volumetric and surface contributions gives unreasonable negative values of C_j , whereas the parallel model in Eq. 15 gives reasonable positive values. The values obtained for C_j per unit mass and the volumetric capacitance per unit mass, on the basis of the parallel model, are shown in Table II. Table II also shows that the volumetric and surface contributions to the capacitance of the solid alumina are similar. The surface contribution decreases with increasing compaction pressure, i.e., decreases with decreasing porosity. This is reasonable, because a decrease in the porosity is expected to be associated with a decrease in the surface area. The frequency has negligible effect on the surface contribution. In contrast, the volumetric contribution is, in essence, not affected by porosity or frequency. This is

Table III. Thermal conductivity of the solid alumina in compacted fumed alumina

Compaction pressure (kPa)	Measured thermal conductivity of compacted alumina [W/(m·K)]	Calculated thermal conductivity of solid alumina [W/(m·K)] ^a
50	—	1.69 ± 0.06
100	—	1.37 ± 0.10
200	0.134 ± 0.003	0.94 ± 0.09

The test pressure was 120 kPa.^aOn the basis of the parallel model.

reasonable, because the volumetric contribution is not expected to depend on the surface area.

Table II also shows the values of κ'' . The values are, in essence, independent of compaction pressure, specimen thickness, and test frequency. This is expected, because of the volumetric nature of κ'' .

Thermal Conductivity

Figure 5b shows a plot of thermal resistivity as a function of specimen thickness for compacted fumed alumina prepared at 200 kPa. The plot is linear. Such linearity is obtained for all the compaction pressures and is in accordance with Eq. 5. The thermal conductivity is related to the reciprocal of the slope of this plot, as described by Eq. 5.

As shown in Table III, the measured thermal conductivity is 0.134 W/(m·K) for the compacted alumina prepared at 200 kPa and tested at 120 kPa. This value is higher than the value previously achieved, 0.08 W/(m·K) for porous carbon-doped silicon oxide with porosity 33% and relatively dielectric constant 2.3.⁶

The thermal conductivity of the solid alumina part of the sample is calculated from the value measured for the compacted fumed alumina, on the basis of the rule of mixtures and known values of the thermal conductivity of bulk alumina [39 W/(m·K)]¹⁶ and air [0.024 W/(m·K)].¹⁷ Both series and parallel models were used, as shown below.

Parallel model:

$$\sigma = v_{\text{alumina}}\sigma_{\text{alumina}} + v_{\text{air}}\sigma_{\text{air}} \quad (17)$$

Series model:

$$\frac{1}{\sigma} = \frac{v_{\text{alumina}}}{\sigma_{\text{alumina}}} + \frac{v_{\text{air}}}{\sigma_{\text{air}}} \quad (18)$$

The series model does not work, because it gives unreasonable negative values for the thermal conductivity of solid alumina whereas the parallel model gives reasonable positive values (Table III). Thus, the value based on the parallel model can serve as the upper bound of the thermal conductivity of the solid alumina in the compacted alumina. This upper bound is much smaller than the

thermal conductivity of bulk alumina [39 W/(m·K)],¹⁶ suggesting that interfaces between the particles in the compacted alumina contribute substantially to the thermal resistance.

Moldability Testing

The fumed alumina powder was compressed at 200 kPa by use of a pin grid array (Fig. 4a–c). As shown in Fig. 4d, the fumed alumina was effectively compacted and held tightly among the pins. Figure 4d shows tight-fitting and uniform distribution of the fumed alumina between the adjacent pins of the pin grid array. The scanning electron microscopy (SEM) image in Fig. 4e shows the structure more clearly; no gaps are apparent at the interface between the fumed alumina and the pin surface.

CONCLUSIONS

In this paper we report a new low- k dielectric material, a new form of porous alumina with pore size mainly <50 nm and relative dielectric constant 2.0 (100 kHz–2 MHz). It was prepared innovatively by compacting aggregates of submicron fumed alumina particles. Both pore size and relative dielectric constant are lower than those previously reported.^{3–5} On compaction at 200 kPa, the fumed alumina aggregates are squashed, resulting in mechanical interconnection among the aggregates and the formation of a nanostructured sheet with porosity 88%. The fumed alumina is moldable by compaction, as shown by the tight fitting of the compacted fumed alumina among the pins of a pin grid array.

The compacted alumina was modeled as solid non-porous alumina and air in parallel (along the direction of dielectric testing), thereby yielding a relative dielectric constant of 9 for the solid alumina. This value is essentially the same as the known value for bulk alumina.

Reducing the compaction pressure from 200 kPa to 50–100 kPa results in greater porosity (92–93%) and slightly higher relative dielectric constant (2.0–2.3) for the compacted alumina, in addition to the substantially higher relative dielectric constant

(13–21) for the solid alumina. The relatively high values of the relative dielectric constant of the solid alumina obtained at the low compaction pressure of 50–100 kPa is because of the increase in the surface capacitance, which is associated with positive surface charges on the fumed alumina. On reducing the compaction pressure, the aggregates are less squashed and the surface charges are probably more exposed, resulting in higher surface capacitance.

For a compaction pressure of 200 kPa, the thermal conductivity of the compacted alumina is 0.134 W/(m·K) and the upper bound of the thermal conductivity of the solid alumina is 0.94 W/(m·K), which is much lower than the value for bulk alumina. The low value of this upper bound suggests that the interface between the alumina particles in the compacted alumina contributes substantially to the thermal resistance. This upper bound is obtained by use of the rule of mixtures, by considering the solid alumina and air to be thermally in parallel (along the direction of thermal testing, which is the same as the direction of dielectric testing).

REFERENCES

1. S. Ma, Y. Wang, Z. Min, and L. Zhong, *Adv. Polym. Technol.* 32, 21358/1 (2013).
2. R. Sasi kumar, M. Ariraman, and M. Alagar, *RSC Adv.* 4, 19127 (2014).
3. S. Lazarouk, S. Katsouba, A. Leshok, A. Demianovich, V. Stanovski, S. Voitech, V. Vysotski, and V. Ponomar, *Microelectron. Eng.* 50, 321 (2000).
4. S. Lazarouka, S. Katsoubaa, A. Demianovichb, V. Stanovskib, S. Voitech, V. Vysotski, and V. Ponomar, *Solid State Electron.* 44, 815 (2000).
5. F. Ito, H. Shobha, M. Tagami, T. Nogami, S. Cohen, Y. Ostrovski, S. Molis, K. Maloney, J. Femiak, and J. Protzman, et al., *Microelectron. Eng.* 92, 62 (2012).
6. M.T. Alam, R.A. Pulavarthy, J. Bielefeld, S.W. King, and M.A. Haque, *J. Electron. Mater.* 43, 746 (2014).
7. S. Wen and D.D.L. Chung, *J. Electron. Packag.* 127, 235 (2005).
8. A. Wang and D.D.L. Chung, *Carbon* 72, 135 (2014).
9. P. Somasundaran, *Encyclopedia of Surface and Colloid Science, 2nd Edition*, Vol. 7 (Boca Raton: CRC Press, 2006), p. 5317.
10. C. Lin and D.D.L. Chung, *J. Mater. Sci.* 42, 9245 (2007).
11. C. Lin and D.D.L. Chung, *J. Electron. Mater.* 38, 2069 (2009).
12. B.C. Daly, H.J. Maris, W.K. Ford, G.A. Antonelli, L. Wong, and E. Andideh, *J. Appl. Phys.* 92, 6005 (2002).
13. H.T. Vo and F.G. Shi, *Microelectron. J.* 33, 409 (2002).
14. http://www.engineeringtoolbox.com/relative-permittivity-d_1660.html. Accessed 9 May 2014.
15. [http://en.wikipedia.org/wiki/Aluminium_oxide_\(data_page\)](http://en.wikipedia.org/wiki/Aluminium_oxide_(data_page)). Accessed 9 May 2014.
16. W.D. Callister Jr and D.G. Rethwisch, *Fundamentals of Materials Science and Engineering*, 4th ed. (Hoboken: Wiley, 2012), p. 850.
17. K.E. Wilkes, R.B. Dinwiddie, and R.S. Graves (eds.), *Thermal Conductivity*, vol. 23 (Boca Raton: CRC press, 1996), p. 604.